Uncovering the gas-, tar- and coke-forming processes in cellulose gasification from the gas phase reactions of levoglucosan as an intermediate

Asuka Fukutome, Haruo Kawamoto*, and Shiro Saka

Abstract: Gas phase pyrolysis of levoglucosan (LG), the major intermediate species during cellulose gasification, was studied experimentally over the temperature range of 400–900 °C. Gaseous LG did not produce any dehydration products, including coke, furans and aromatic substances, although these are characteristic products of pyrolysis of molten LG. Alternatively, at >500 °C, gaseous LG produced only fragmentation products, such as noncondensable gases and condensable C1-C3 fragments as intermediates during noncondensable gas formation. Therefore, it was determined that secondary reactions of gaseous LG can result in clean (tar- and coke-free) gasification of cellulose. Cooling of remaining LG in the gas phase caused coke formation by transitioning the LG to the molten state. The molecular mechanisms that govern the gas and molten phase reactions of LG are discussed in terms of the acid catalyst effect of intermolecular hydrogen bonding promoting the molten phase dehydration reactions.

Introduction

Gasification is a promising technology for the conversion of biomass resources into biofuels and biochemicals. The gases generated by this process can be utilized for power generation and the production of synthetic petroleum and chemicals via the Fischer–Tropsch (FT) synthesis. Issues related to tar formation, however, represent a challenge that must be solved to allow the establishment of reliable systems. This is required since tar causes clogging of the gasifier outlet and can damage engines and turbines used for power generation by condensing and coking on walls. Coking by tar materials also deactivates FT catalysts. An improved understanding of the chemistry involved in biomass gasification would therefore assist in upgrading existing gasification processes to produce cleaner gases.

Biomass gasification proceeds as a two stage process, consisting of a primary pyrolysis step to form volatiles and solid char materials and the secondary reactions of these primary products.[1] Coking, which forms solid carbonaceous residues, represents a secondary reaction of the volatile materials.

Hosoya et al.[2] have studied the coking behavior of cellulose, which is a major component of wood and other

A. Fukutome, Prof. Dr. H. Kawamoto, Prof. Dr. S. Saka
Graduate school of Energy Science.
Yoshida-honmachi, Sakyo-ku, Kyoto 606-8501 (Japan)
E-mail: kawamoto@energy.kyoto-u.ac.jp

lignocellulosic biomass resources, in Pyrex glass tubes under nitrogen at 800 °C. Coking was observed primarily following the condensation of volatile intermediates on the reactor walls at lower temperatures. Thus, coking reactions were determined to occur subsequent to cooling of the gaseous volatile intermediates during cellulose gasification, leading to clogging of the pipeline from the gasifier. Later, Fukutome et al.[3] compared the coking behaviors of various cellulose-derived volatile intermediates in a Pyrex glass ampoule under nitrogen at 600 °C. Levoglucosan (LG), glycolaldehyde, furfural and 5-hydroxymethylfurfural (5-HMF) were found to form coke in the molten state before vaporization. Thus, these intermediates were believed to contribute to the coking process after condensation. These findings led to a hypothesis; the gas-phase secondary reactions of cellulose-derived volatile intermediates such as LG and glycolaldehyde do not generate tar and coke during gasification, but rather it is molten phase reactions that produce coke.

LG is the primary intermediate product of cellulose pyrolysis.[4] Kwon et al.[5] and Shafizadeh et al.[4e] have reported LG yields as high as 70.1% and 58%, respectively, from the pyrolysis of cellulose under vacuum in the temperature range from 400 to 430 °C. Many papers[4b, 6] have concluded that the chemical compositions of the pyrolysis products are similar for both LG and cellulose. Thus, the pyrolysis reactions of LG have been extensively studied so as to better understand cellulose pyrolysis.[4b, 6c, 7] In the molten state, the condensation of LG through transglycosylation reactions has its onset at approximately 230–250 °C,[7a-c, 7f, 7g, 7i] a range that is much lower than the boiling point of LG (385 °C[8]) and the formation temperatures of LG from cellulose (>300–350 °C[9]). Based on these results, the relative evaporation/condensation efficiency of LG has been suggested as the main factor determining the selectivity for volatiles/char in cellulose pyrolysis.[7i, 10] However, only a few studies[7h, 7k] have focused on the gas-phase reactions of LG.

The vapor-phase secondary reactions of the volatile products from wood[1b-e] and cellulose[1a, 1b, 1f, 11] have been studied using two-stage experimental setups consisting of primary and secondary pyrolysis reactors. Evans and Milne[1b] reported variations in the product compositions obtained from the vapor phase secondary reactions of the volatile products of wood and its constituent polymers by direct analysis with a molecular-beam mass spectrometer. Using a similar system, Shin et al.[7h] reported the vapor-phase conversion of LG and other cellulose-derived primary products in the temperature range of 500 to 700 °C. However, their work does not, strictly speaking, deal with the gas-phase reactions of LG, because the

polymerization and other molten phase reactions of LG occur at temperatures above 230–250 °C, and so take place before complete vaporization. Therefore, products from the molten-phase reactions of LG may be included in the gas phase secondary reactions stage. Hosoya et al.[7k] compared the reactivities of molten and gas phase LG, using a dual space ampoule reactor at 400 °C, and found that gaseous LG selectively produced CO and CO_2, in contrast to the formation of coke and other low molecular weight products in the molten state. These results encouraged us to further investigate the gas phase reactions of LG to address the above hypothesis.

In this paper, we report the gas phase secondary reactions of LG as studied using a flow-type two-stage tubular reactor including an evaporator. The data are compared with those obtained by the molten phase pyrolysis of LG so as to characterize the gas phase reactions. Finally, the associated molecular mechanisms of cellulose gasification are discussed, focusing on the tar and coke formation arising from the different reactivities in the gas and molten phases.

Results and Discussion

Figure 1 illustrates the two-stage tubular reactor. In this device, a quantity of LG inserted in the quartz glass tube of the evaporator was heated under a nitrogen flow of 400 ml/min. The temperature of the evaporator was carefully controlled in the vicinity of 200 °C, a temperature between the LG melting point (185 °C) and the onset temperature (approximately 250 °C) at which the condensation and other molten phase reactions of LG occur. With this system, the LG was completely vaporized without decomposition and then fed into the pyrolyzer. This was confirmed by the analysis of the recovered substances using gel permeation chromatography (GPC) (column: Asahipac GS-220HQ) without heating at the pyrolyzer.
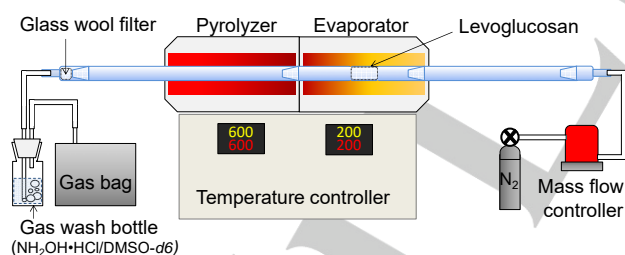

Figure 1. Flow-type two-stage tubular reactor consisting of a levoglucosan evaporator connected to a pyrolyzer and product recovery units.

The gaseous LG was heated in the temperature range of 400 to 900 °C within the pyrolyzer, and the resulting pyrolyzates were recovered as condensable and noncondensable substances. Unreacted LG and the condensable products were obtained from two regions: on the walls of the cooling line leading from the pyrolyzer and in a DMSO-d_6 solution containing an oximation reagent ($NH_2OH \cdot HCl$) in a gas wash bottle. These are referred to as the high and low boiling point (bp) fractions, respectively, in this paper. Some products with relatively low boiling points did not condense on the walls of the cooling line and were instead captured in the gas wash bottle, where aldehydes/ketones and ketene were effectively converted into the corresponding less volatile aldoximes/ketoximes (cis/trans isomers) and N-acetylhydroxyamine, respectively (Scheme 1). The noncondensable gases were collected in a gas bag.
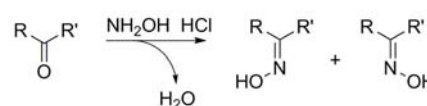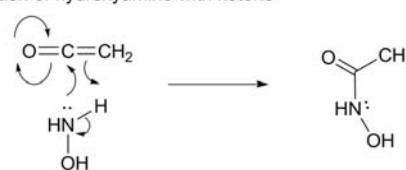
Scheme 1. The derivatization of aldehydes, ketones and ketene with hydroxylammonium chloride as an oximation reagent in the gas wash bottle.
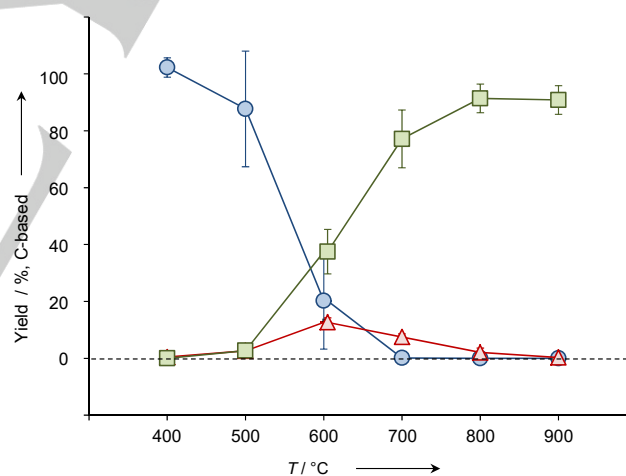

Figure 2. Recoveries (%, C-based) of levoglucosan (LG) and yields (%, C-based) of the condensable products and non-condensable gases during the pyrolysis of gaseous LG at 400 to 900 °C with residence times of 0.8 to 1.4 s under a N_2 flow of 400 ml/min. Legend: ○, recovery of LG; △, condensable products; □, non-condensable gases. The error bars represent 95% confidence intervals caculated with the standard deviation of the three replicates

Figure 2 shows the C-based yields (%) of the condensable and noncondensable products from the pyrolysis of gaseous LG at residence times from 0.8 to 1.4 s and at temperatures between 400 and 900 °C. Error bars show the 95% confidence intervals (1.96×standard deviation of the three replicates).

Although the molten LG has been pyrolyzed at temperatures as low as 250 °C,[7m] pyrolytic decomposition of the gaseous LG started at 500 °C and became more pronounced in the temperature range of 600 to 700 °C. By increasing the temperature to 900 °C, the LG could be almost completely converted into noncondensable gases. Evans and Milne[1b] have also reported such unexpected stability for gaseous LG. The condensable products formed in relatively high yields at the mid-range temperatures of 600 and 700 °C, where the yields amounted to 13.7±1.7 and 8.1±1.3% (C-based), respectively. Only very small amounts of condensable products [0.2±0.1% (C-based)] were detected at 900 °C. Thus, the condensable products were evidently relatively stable intermediates in the conversion from LG to noncondensable gases. When the yields of condensable products are higher, the mass balances were below 100%. Especially at 600 °C, the mass balance was only 66.5±11.3%. The loss of carbon is probably caused by the evaporation of condensable products. We observed the evaporation of products with lower bp such as methanol, acetone, and formaldehyde during the further bubbling process of N_2 to the solutions. Furthermore, protons in aldehyde group may be slightly exchanged with deuterium in DMSO-*d6*, which would led further underestimation of the amount of aldehydes,

No coke or colored substances were detected anywhere in the experimental setup during these trials. All the condensates found in the cooling line from the pyrolyzer at each temperature were completely recovered as colorless solutions by extraction with DMSO-d_6.

1. Condensable products

The identities of the condensable products were determined from their ^{1}H-NMR spectra by comparison with those of reference compounds. Examples of the spectra of the high and low bp fractions obtained from the pyrolysis of gaseous LG at 600 °C (residence time 1.1 s) are shown in Figure 3 (a) and (b), respectively. An enlarged spectrum of the low bp fraction with the identification of the signals is presented in Figure 4 (a), along with the spectrum obtained from the pyrolysis of molten LG under nitrogen at 350 °C over 5 min for comparison.
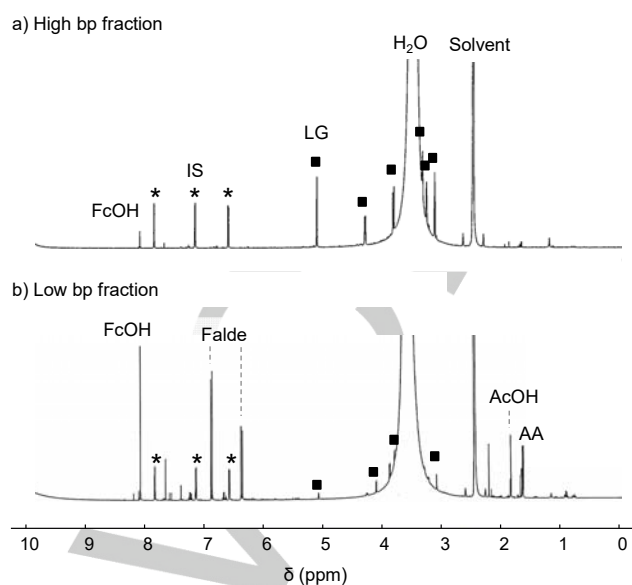

Figure 3. ^{1}H-NMR spectra of a) high and b) low boiling point (bp) condensable fractions obtained from the pyrolysis of gaseous levoglucosan at 600 °C with a residence time of 1.1 s under a N_2 flow of 400 ml/min. Legend: FcOH, formic acid; Falde, formaldehyde; LG, levoglucosan; AcOH, acetic acid; AA, acetaldehyde; ■, signals assigned to LG.

No high molecular mass refractory tars were detected, although the literature[1b, 11] indicates the formation of such compounds during the gas-phase secondary reactions of cellulose pyrolysis. The high bp fractions obtained at all temperatures applied in this study were completely soluble in water and did not include any products with higher molecular masses than LG, as determined by GPC analysis. The NMR spectrum peaks [Figure 3 (a)] was also assigned to LG and lower molecular mass products, such as formic acid, all of that were also observed in the low bp fraction. No polymerization products of LG were detected even after the condensation on the walls of the cooling line. This is attributed to the nitrogen flow applied in these experiments, which was able to transport the LG to surfaces with temperatures lower than the LG polymerization temperature of 250 °C.

As indicated from the assignments of the NMR signals in Figure 4 (a), the low bp fractions were found to include C1–C3 fragmentation products, such as aldehydes (formaldehyde, acetaldehyde, glycolaldehyde, glyoxal, methylglyoxal and acrolein), ketones (hydroxyacetone and acetone), acids (formic acid and acetic acid), alcohol (methanol) and ketene. The yields (%, C-based) of the condensable products are shown in Figure 5 as a function of the temperature of the pyrolyzer. Error bars show the 95% confidence intervals (1.96×standard deviation of the three replicates). Methanol, formaldehyde, and acetone etc. with relatively low boiling points, tended to evaporate from the gas wash bottle, and this may have led to the underestimation of the yield of these products with low bp in this system. Products with more than four carbons (C4) were not detected at all. The C3 products methylglyoxal, acrolein, hydroxyacetone and acetone were identified, although their yields were relatively low

compared with those of the C1 and C2 products. Thus, C1 and C2 aldehydes/acids accounted for the majority of the condensable products.

The compositions of the condensable products varied depending on the temperature of the pyrolyzer. The yields of formic acid, glyoxal and methylglyoxal reached their maximum values at 600 °C and then decreased sharply at 700 °C. This pronounced temperature dependency likely arises from the lability of these products at 700 °C. Formic acid is known to decompose into CO_2, H_2, CO and H_2O as low as 250 °C,[3, 12] while glyoxal is reported to decompose into formaldehyde and CO at 450 °C.[13] Accordingly, the formation of formic acid, glyoxal and methylglyoxal from gaseous LG are likely to be the rate determining steps for the conversion of LG into noncondensable gases at temperatures higher than 700 °C.

In contrast, acetaldehyde and ketene exhibited peak yields at higher temperatures of 700 and 800 °C, respectively. Because LG completely disappeared at 700 °C, these products appear to have been formed through secondary reactions of the intermediates generated by gaseous LG. Ketene is reported to form from acetic acid[14] during pyrolysis, and this is supported by the acetic acid and ketene yield trends in Figure 5. Although

details of these reaction pathways are not known, Asmadi et al.[15] have reported that the formation of acetaldehyde from wood samples was delayed during pyrolysis at 600 °C.

A kind of dehydration reaction, leading to the formation of furfural, 5-HMF and coke, is known to proceed during the pyrolysis of molten LG. In fact, several signals assigned to furfural and 5-HMF were clearly observed in the NMR spectrum resulting from the pyrolysis of molten LG [Figure 4 (b)], along with the formation of coke and polymerization products. Interestingly, no signals assignable to furans were observed in the spectra resulting from gaseous LG [Figures 3 and 4 (a)].

Accordingly, by maintaining the LG strictly in the gas phase, the fragmentation reactions were selectively promoted rather than the polymerization (transglycosylation) and dehydration reactions. These results suggest that the transglycosylation and dehydration reactions are characteristic of the molten phase pyrolysis of LG and other carbohydrates. Molecular mechanisms associated with the molten and gas phase pyrolysis reactions are discussed further on, in terms of the hydrogen bonding formed in the molten state.

The results of the present study also provide insights into the pyrolytic formation of several products from LG and cellulose.
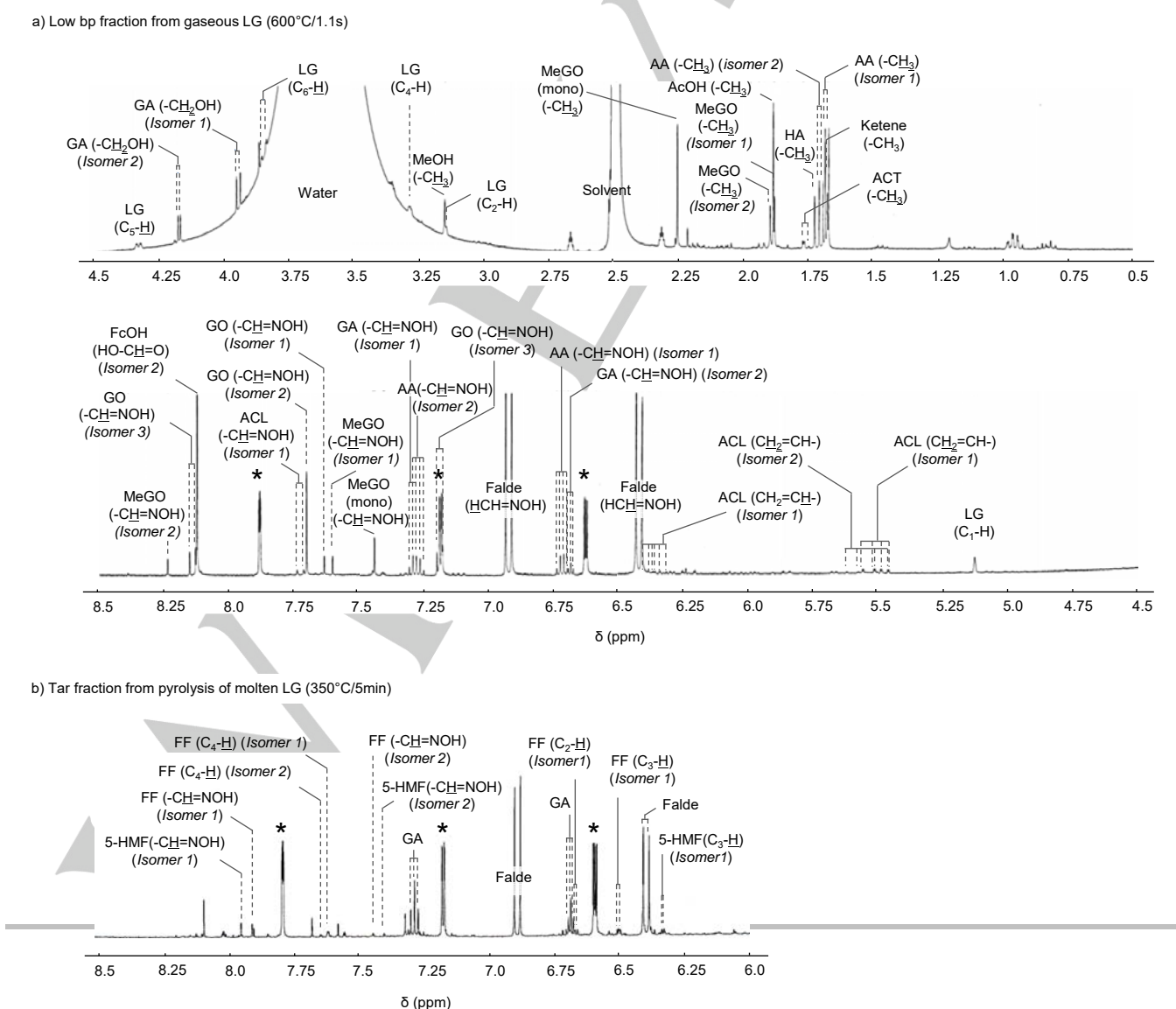
a) Low bp fraction from gaseous LG (600°C/1.1s)

b) Tar fraction from pyrolysis of molten LG (350°C/5min)

Figure 4. Signal assignments for the ^{1}H-NMR spectrum of (a) the low boiling point fraction obtained from the pyrolysis of gaseous levoglucosan (LG) at 600 °C with a residence time of 1.1 s under a N_2 flow of 400 ml/min and (b) the pyrolysis products from molten LG at 350 °C over 5 min. Legend: AA, acetaldehyde; ACL, acrolein; ACT, acetone; AcOH, acetic acid; Falde, formaldehyde; FcOH, formic acid; FF, furfural; 5-HMF, 5-hydroxymethylfurfural; GA, glycolaldehyde; GO, glyoxal; HA, hydroxyacetone; MeGO, methyl glyoxal; MeGO(mono), methyl glyoxal mono oximised.; * signals assigned to 2-furoic acid (internal standard).

Hydroxyacetone, which is a typical product of the pyrolysis of molten LG,[7e, 7k] was generated in only minimal quantities from the gaseous LG, and hence this compound would tend to be formed selectively by the molten phase reactions of LG. Literature reports[16] have proposed the competitive formation of glycolaldehyde and LG during the primary pyrolysis stage of cellulose. However, the present study clearly observed the formation of glycolaldehyde from the gas phase pyrolysis of LG, indicating that at least a secondary reaction pathway exists for the formation of glycolaldehyde from cellulose.

2. Noncondensable gases

The major components of the noncondensable gases were determined to be CO, H_2, CO_2, ethylene, acetylene and methane, along with ethane, propane and propylene as minor components. Yields (C-based %) and compositions (mol %) of these gases are shown in Figure 6 and Table 1, respectively, as functions of the temperature of the pyrolyzer. Error bars show the 95% confidence intervals (1.96×standard deviation of the three replicates). These gases may be categorized as oxygenated or hydrocarbon gases and H_2. The hydrocarbon gas concentrations were normally low, in the range of 4.3–13.6 mol %, reaching a maximum at 800 °C, while the oxygenated gases and H_2 accounted for 64.5–90.3 and 5.3–25.1 mol %, respectively.
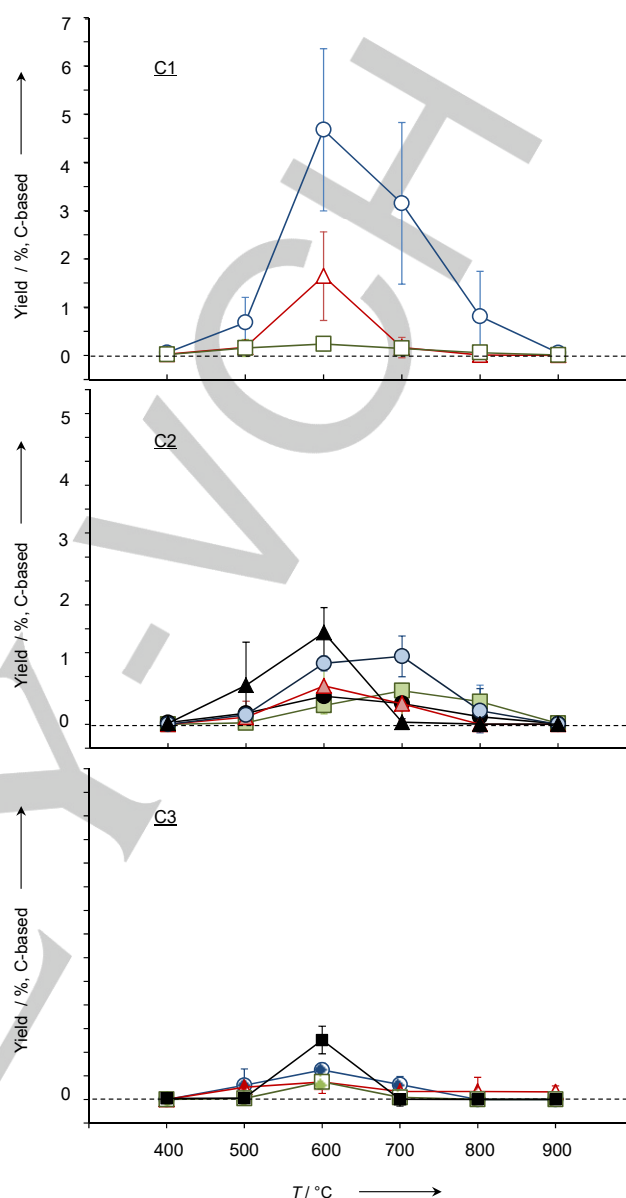

Figure 5. Yields (%, C-based) of the condensable products obtained from the pyrolysis of gaseous levoglucosan at 400 to 900 °C with residence times of 0.8–1.4 s under a N_2 flow of 400 ml/min. Legend: ○, formaldehyde; △, formic acid; □, methanol; ▲, glyoxal; ●(light blue), acetaldehyde; △(red), glycolaldehyde; □(green), ketene; ●, acetic acid; ●(blue), acrolein; △(red), acetone; ●(green), hydroxyacetone; ■, methylglyoxal. The error bars represent 95% confidence intervals calculated with the standard deviation of the three replicates
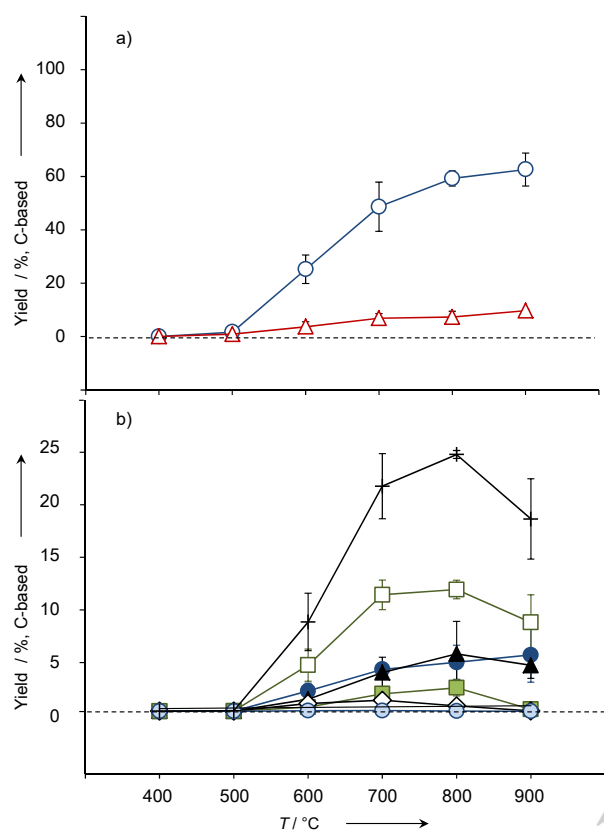
Figure 6. Yields (%, C-based) of (a) oxygenated and (b) hydrocarbon gases obtained from the pyrolysis of gaseous levoglucosan at 400 to 900 °C with residence times of 0.8 to 1.4 s under a N_2 flow of 400 ml/min. Legend: ○, CO; △, CO_2; +, hydrocarbon gases (total);, □C_2H_4; ●, C_2H_2; ▲, CH_4; ■, C_2H_6; ◇, C_3H_6; ●, C_3H_8. The error bars represent 95% confidence intervals calculated with the standard deviation of the three replicates

Production of the noncondensable gases started at 500 °C, as was also observed in the case of the condensable products, although the yield at that point was only 2.6%±1.9%. The oxygenated gases (CO and CO_2) were predominant (90.3 mol %) at 500 °C. The proportion of these oxygenated compounds, however, decreased to 70.3 mol % at 600 °C, since the concentrations of products other than CO_2 were increased significantly by raising the temperature from 500 to 600 °C. This observation is consistent with literature reports[17] that CO_2 is preferentially formed at relatively low pyrolysis temperatures. In the temperature range of 600–800 °C, the gas compositions did not change greatly, even though the gas yield significantly increased. These results indicate that similar gas formation mechanisms are involved in this temperature range. At 900 °C, the hydrocarbon gas content decreased, and this phenomenon will be discussed further on.

Saturated hydrocarbon gases with more than three carbons were almost negligible at all temperatures in this study. Methane (2.4–4.1 mol %) and ethane (0–1.2 mol %) were found, but the effects of the pyrolysis temperature were different in both cases. Methane was usually observed as the major saturated

hydrocarbon gas even at the lowest temperature of 500 °C, while ethane started to form at 600 °C (0.6 mol %) and its proportion increased to 1.2 mol % at 700 and 800 °C with a sharp decrease to 0.1 mol % at 900 °C.

Table 1. Proportions (mol %) of non-condensable gases obtained from the pyrolysis of gaseous levoglucosan at 500 to 900 °C with residence times of 0.80 to 1.4 s under a N_2 flow of 400 ml/min.

	Pyrolysis temperature [°C]				
	500	600	700	800	900
H_2	5.3	17.0	20.5	21.8	25.1
Oxygenated gas	**90.3**	**70.3**	**66.1**	**54.5**	**65.4**
CO	63.8	64.1	59.5	56.9	56.9
CO_2	26.5	6.2	6.6	7.6	8.5
Hydrocarbon gas	**4.3**	**12.6**	**13.4**	**13.6**	**9.6**
CH_4	2.4	2.6	3.7	4.1	3.5
C_2H_6	0.0	0.6	1.2	1.2	0.1
C_3H_8	0.0	0.1	0.0	0.0	0.0
C_2H_4	1.0	5.8	5.9	5.7	2.9
C_3H_6	0.0	0.7	0.4	0.1	0.0
C_2H_2	0.9	2.8	2.2	2.5	3.1
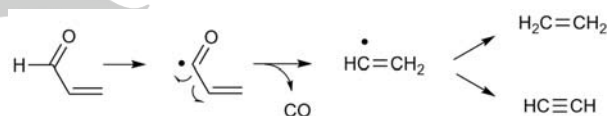
Scheme 2. Pathways for the formation of ethylene and acetylene from acrolein.
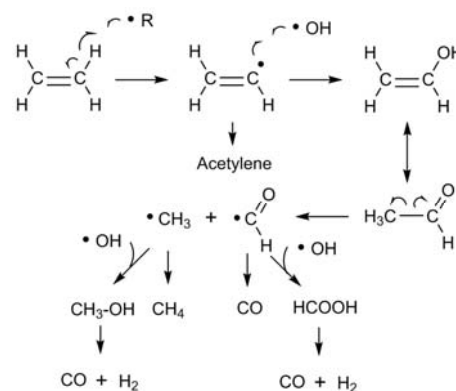
Scheme 3. Possible reactions during the conversion of ethylene to acetylene, oxygenated gases and hydrogen at 900 °C.

These results could be explained by supposing that methane forms over the course of the fragmentation reactions of gaseous LG via the methyl radical. The formation of methane from acetic acid is a well-known reaction in pyrolysis.[14, 18]

Contrary to this, ethane formation would involve a pathway including hydrogen addition to ethylene, along with the coupling of two methyl radicals, and ethylene was produced even at the lowest temperature of 500 °C. As shown in the reaction scheme in Scheme 2, the α-scission reaction of the acrolein radical forms the vinyl radical, which is further converted into ethylene[19] and acetylene by hydrogen abstraction and β-scission reactions, respectively. The hydrogen radical concentration would be increased when raising the temperature from 500 to 600 °C, as indicated by the H_2 yield trend, and this could enhance the formation of ethane. The sharp decrease in the ethane concentration at 900 °C results from the instability of the C–C bond when subjected to homolysis, generating methane via the resulting methyl radicals. Methane, with only the stronger C–H bonds, is more stable than ethane.

Unsaturated hydrocarbons, whose C=C and C–H bonds are resistant to homolysis and hydrogen abstraction reactions, respectively, represented the remaining hydrocarbon gases (ethylene: 1.0–5.9 mol %; and acetylene: 0.9–3.1 mol %). The ethylene and acetylene yields attained their maximum values at 800 °C (11.7±0.9%, C-based) and 900 °C (5.4±2.6 %, C-based), respectively. Similar levels of ethylene have also been reported to form during the fast pyrolysis of cellulose at 850 °C with a short residence time of 0.3 s.[20]

When increasing the temperature from 800 to 900 °C, the ethylene content decreased from 5.7 to 2.9 mol %. Together with the decrease in the ethane content, this contributed to the decrease in the hydrocarbon gas content from 13.6 mol % (800 °C) to 9.6 mol % (900 °C). Alternatively, the levels of oxygenated gases, H_2 and acetylene increased in this temperature range. Accordingly, ethylene evidently was converted into these gases at 900 °C. This is also supported by the O-based yields of the products, which increased from 92.6 % at 800 °C to approximately 100 % at 900 °C. This change would involve the oxidation of ethylene, as shown in the proposed pathways in Scheme 3. At the higher temperature, the hydrogen abstraction reaction of C–H bonds occurs to only a minor degree, and vinyl hydrogens would be abstracted by radical species to form vinyl radicals, possibly leading to the formation of more labile oxygenated intermediates by coupling with oxygen-centered radicals such as •OH. These reactions promote the formation of oxygenated gases and H_2. Acetylene is also formed from these vinyl radical intermediates.

Details of the decomposition mechanisms of gaseous LG will be presented in a forthcoming paper,[21] but we suggest here that homolysis along with several radical chain reactions can explain the fragmentation reactions that eventually result in the formation of the noncondensable gases. With this mechanism in mind, the preferential formation of oxygenated gases over hydrocarbon gases can be understood on the basis of the initial reactions presented in Scheme 4.
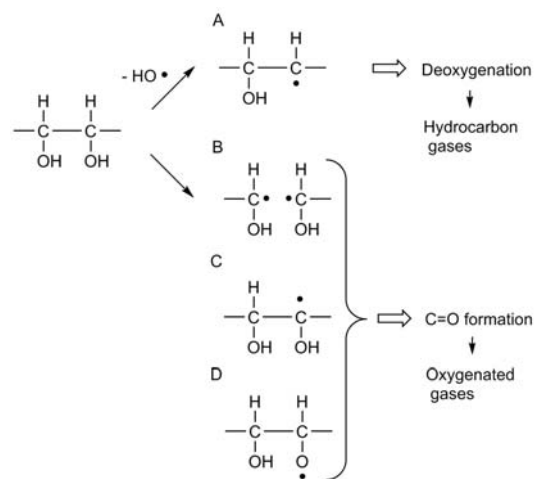

Scheme 4. Formation of intermediate radicals through the homolysis and abstraction of hydrogen atoms responsible for selectivity between hydrocarbon and oxygenated gases from gaseous levoglucosan.

The production of hydrocarbon gases from LG requires a deoxygenation step. Direct homolysis of the C–O bonds forms radical (A), which subsequently generates an olefinic structure by the elimination of the OH group through a β-scission reaction. However, the bond dissociation energies of C–OH bonds are normally higher than those of the corresponding C–C bonds, and hence the formation of radical (B) is preferred during the homolysis process. Additionally, radicals (C) and (D) can formed by the hydrogen abstraction reactions of the C–H and O–H moieties, respectively. These radicals (B), (C) and (D) result in the formation of aldehydes and ketones that are further converted into CO and CO_2. The aldehydes in particular are expected to be converted into CO and CO_2 via the aldehyde radicals shown in Scheme 5.
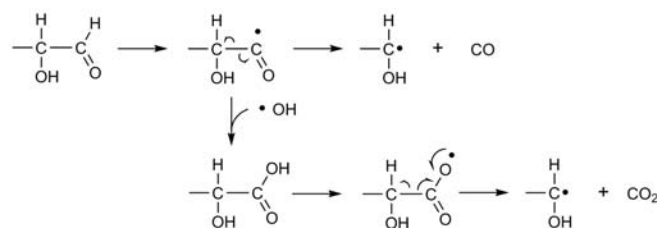
Scheme 5. Possible pathways from aldehydes to CO and CO_2.

3. Molecular mechanisms governing the gas and molten phase reactions
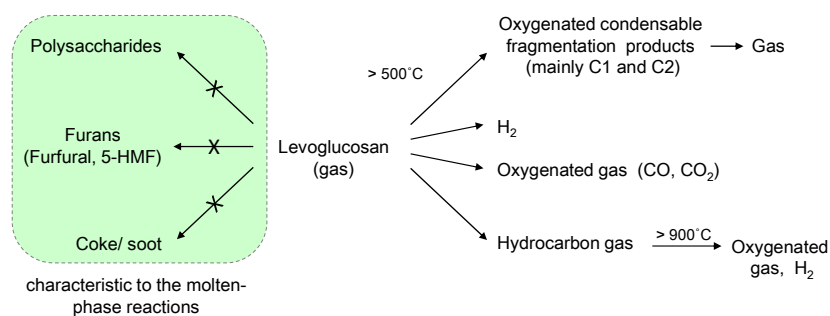
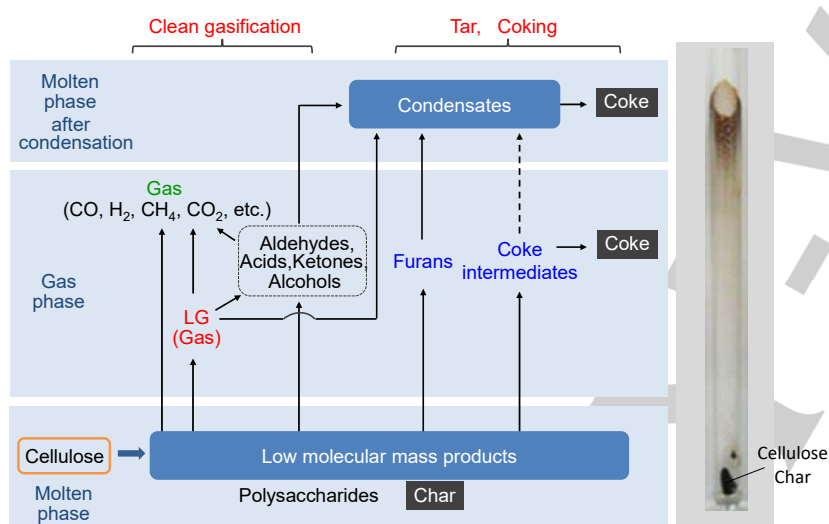**Scheme 6.** Summary of the pyrolytic conversion of gaseous levoglucosan.

Figure 7. Proposed steps in the gas-phase reactions of levoglucosan (LG) along with the tar and coke formation mechanisms in cellulose gasification. Image: coke formation following cellulose pyrolysis in a glass tube with a temperature gradient from 800 °C (bottom) to room temperature (upper end of the tube).[2]

As summarized in Scheme 6, gaseous LG was found to generate only fragmentation products and, eventually, noncondensable gases at temperatures above 500 °C. Interestingly, the dehydration reactions that lead to the formation of furans and coke/soot were not observed during the gas-phase pyrolysis of LG, and hence these reactions are believed to be unique to the molten phase pyrolysis, along with the transglycosylation reactions. Because the carbonaceous products consist primarily of benzene ring compounds, coke and soot formation can be considered as a kind of aromatization process to form benzene rings. An interesting proposal has been made for the formation mechanism of carbonaceous products based on benzene rings in the literature[22] that includes the polymerization of furan precursors, followed by rearrangement

As shown in the photographic image of the reactor (Figure 7) after the pyrolysis of cellulose at 800 °C under nitrogen, followed by tar-extraction,[2] large amounts of coke were formed in the molten phase secondary reactions stage. This coke formation is attributed to the reactivity change caused by the

from furan to benzene rings. This indicates that the furan formation and the coke/soot formation in Scheme 6 are closely related to each other in terms of the aromatization reactions that form furan and benzene rings through dehydration reactions.

The resistance of gaseous LG to pyrolytic decomposition up to 500 °C strongly indicates that the activation mechanisms only occur during molten phase pyrolysis, since the molten phase reactions of LG normally occur at 250 °C. Kawamoto's group has proposed a hydrogen bond theory for the activation mechanisms of molten state carbohydrates including LG, based on the unexpected stability observed in proton acceptor solvents such as aromatics[7j, 23] and polyethers.[7m, 23-24] In this theory, intermolecular hydrogen bonding between carbohydrate molecules mimics the actions of acid and base catalysts at elevated temperatures. With this form of acid catalysis, dehydration and transglycosylation reactions can proceed at lower temperatures in molten carbohydrates. The stability of gaseous LG is explained by this theory, since the occurrence of such activation mechanisms through intermolecular hydrogen bonding is not expected in the case of gaseous LG.

4. Roles of gas and liquid phase reactions in cellulose gasification

The nature of the gas phase reactivity of LG provides insight into the gasification mechanism of cellulose in terms of the effects of phase transition (Figure 7). Cellulose gasification occurs in a sequential three stage process, involving a primary molten phase pyrolysis stage followed by gas and molten phase secondary reactions.

Depolymerization and other pyrolysis reactions occur in the molten phase formed at the surface of cellulose crystallites in the temperature range of 300–450 °C.[8, 25] Some of the resulting low MW products, including LG, evaporate into the gas phase, while the others are re-polymerized and eventually converted into carbonaceous material (char) via dehydration reactions. The coke-forming behavior of cellulose is discussed below, based on the reactivity of LG as the major volatile product and changes brought about by the phase transition from the gas to molten phase.

transition from the gas to molten phase, where the dehydration and transglycosylation reactions become effective even at lower temperatures. In contrast, gaseous LG and decomposition products (primarily C1 and C2 fragmentation products) were found to be cleanly gasified without forming tar

or coke when the residence time was sufficient to complete the gasification.

Cellulose gasification also produced coke during the gas phase secondary reactions stage, although to a lesser extent (Figure 7). Fukutome et al.[3] identified furans (furfural and 5-HMF) as the potential precursors of this type of coke formation by studying the coke-forming reactivities of eight major volatile products of cellulose in closed ampoules at 600 °C. However, gaseous furans are reported to be stable up to approximately 800 °C.[26] These results suggest that this type of coke is produced via the volatile intermediates formed from the molten phase reactions of furans during the primary pyrolysis stage of cellulose. These same intermediates are not produced by the gas phase reactions of LG. For this reason, the gas phase reactions of LG are also clean in terms of lack of coking in the gas phase.

In actual biomass gasification, LG would be exposed to the volatiles derived from the other components such as lignin, which will alter the reactivity of LG. Hosoya et.al. [27] examined the interactions between cellulose volatiles and lignin volatiles with a dual spaced ampoule reactor at 600 °C. They concluded that the lignin volatiles enhanced the gasification of cellulose volatiles, while coke formation from those lignin volatiles was inhibited. They suggested that lignin volatiles are usually obtained as radicals and those radicals are stabilized by the abstraction of proton from cellulose volatiles, which also enhance the fragmentation of cellulose volatiles. However, the interaction of LG itself with lignin volatiles has not been studied yet. Further studies are needed,

Experimental Section

Two-stage tubular reactor

The two-stage tubular reactor (Figure 1) used in this study consisted of two electric cylindrical furnaces (internal diameter: 35 mm, length: 160 mm, Asahi Rika Seisakusho Co., Ltd.), serving as the evaporator and pyrolyzer. Each furnace included a quartz glass tube (internal diameter: 15 mm, wall thickness: 1.5 mm), and these were connected to one another. The tube used in the evaporator had two fringes set 30 mm apart to allow the application of LG to the desired area. The right end of the evaporator was attached to a nitrogen cylinder via a mass flow controller (Horiba SEC-400MK3), and the other end, coming from the pyrolyzer, was connected to a gas wash bottle via a glass wool filter and then to a gas bag. Air flow was supplied to the outer part of the tube coming from the pyrolyzer to quench the pyrolysis reactions. A DMSO-d_6 solution (2.0 ml) containing an oximation reagent (NH$_2$OH•HCl) (20 mg) was placed in the gas wash bottle to recover the volatile products.

Pyrolysis

A solution of LG (15 mg, Carbosynth Ltd., Berkshire, UK) in methanol (0.20 ml) was applied to the area separated by the fringes in the evaporator tube, after which the methanol was evaporated under a

Conclusions

The gas phase pyrolysis of LG was studied in a two-stage tubular reactor during the evaporation of LG under a nitrogen flow at 400–900 °C, applying residence times of 0.8–1.4 s. The following results were obtained.

1. LG in the gas phase was much more stable during pyrolysis than in the molten state.
2. The stability of gaseous LG was explained by the associated lack of intermolecular hydrogen bonding that otherwise can mimic the effects of acid and base catalysts.
3. The gas phase pyrolysis of LG selectively generated fragmentation products at temperatures above 500 °C. No dehydration products (furans and coke) or transglycosylation (polymerization) products were detected under these conditions. Thus, these products are believed to be unique to the pyrolysis of molten LG.
4. The coke formation behavior of cellulose can be reasonably explained by considering the different reactivities of LG in the gas and molten phases. Substantial coke formation occurred upon cooling of the remaining LG to form the molten phase, in which intermolecular hydrogen bonding becomes effective and serves as an acid catalyst to promote the transglycosylation and dehydration reactions even at lower temperatures.
5. The gas phase reactions of LG were found to contribute to the tar- and coke-free gasification, producing cleaner gases. Conversely, the molten phase reactions result in tar and coke formation.
6. The precursors that react to form coke in the gas phase appear to originate from the molten phase reactions during cellulose pyrolysis.

nitrogen flow and the tube was completely dried in a desiccator under vacuum. A nitrogen flow (400 ml/min) was supplied for 30 min prior to conducting each pyrolysis trial so as to sweep out the air inside the reactor. The pyrolyzer was preheated at the designated temperature (between 400 and 900 °C), the evaporator was heated to 120 °C over 5 min and this temperature was maintained for an additional 5 min. The evaporator was subsequently heated to 200 °C at 16 °C/min. When the temperature reached approximately 185 °C, the LG melted and began to vaporize. After holding the evaporator at 200 °C for 5 min, heating was stopped and the tube reactor was cooled by opening the furnace covers and subsequently applying an air flow. The nitrogen flow was maintained for an additional 2 min to sweep any residuals products into the gas wash bottle and gas bag.

The residence time of the pyrolyzer was defined as the period over which the gaseous substances were present in the region of the pyrolyzer with temperatures within the set value ±25 °C. The internal temperature profiles of the pyrolyzer and evaporator were obtained for each set temperature by direct measurement during preliminary control trials conducted without the addition of LG. A constant nitrogen flow of 400 ml/min was supplied during each experimental trial, and hence the residence time changed depending on the temperature of the pyrolyzer. The residences times at 400, 500, 600, 700, 800 and 900 °C were determined to be 1.4, 1.2, 1.1, 1.0, 0.87 and 0.80 s. The pressure inside the reactor was measured and was found to equal atmospheric pressure.

Molten phase pyrolysis

Levoglucosan was placed at the bottom of a Pyrex glass tube reactor (internal diameter: 8.0 mm, thickness: 1.0 mm, length: 300 mm). After the air inside the reactor was replaced with N₂ by using an aspirator connecting through a three-way tap, the reactor was inserted into a muffle furnace preheated at 350 °C through a small hole of the top of the furnace. After heating for 5 min, the reactor was taken out and immediately cooled with flowing air (30 s) and then in cold water (30 s)

Product analysis

The condensates on the reactor tube wall and the line between the reactor and the gas wash bottle were rinsed off with DMSO-d_6 (2.0 ml) to obtain the high bp fractions. Low bp fractions were obtained from the gas wash bottle as the DMSO-d_6 solutions. These solutions were directly analyzed by ¹H-NMR spectroscopy using a Brucker AC-400 (400 MHz) spectrometer following the addition of 2-furoic acid as an internal standard. Quantification of the products along with the recovered LG was performed based on the peak areas of the NMR signals as compared with those of the internal standard.

The noncondensable gases other than acetylene were determined by micro GC with a Varian CP-4900 instrument, under the following chromatographic conditions: channel (1) column: MS5A 10 m; carrier gas: Ar; column temperature: 100 °C; column pressure: 170 kPa; detector: thermal conductivity detector (TCD); retention times (s): H_2 (26.4), N_2 (45.7), O_2 (35.4), CH_4 (60.6), and CO (86.9); channel (2) column: PoraPLOT Q 10 m; carrier gas: He; column temperature: 80 °C; column pressure: 190 kPa; detector: TCD; retention time (s): CO_2 (19.9), C_2H_4 (23.5), C_2H_6 (26.3), C_3H_6 (57.4) and C_3H_8 (63.2). Quantification of acetylene was conducted by GC with a Shimadzu GC-14B instrument under the following chromatographic conditions: column: RESTEC, Rt@-Alumina BOND/N₂SO₄ (30 m, 0.53 mm Ø), carrier gas: He, column temperature: 60 °C (0–2 min), 40–200 °C (2–16 min, 10 °C/min), 200 °C (16–20 min); detector: flame ionization detector; retention time of acetylene: 4.3 min.

Acknowledgements

Keywords: Biomass • Gas-phase reactions • cellulose • gasification • levoglucosan

[1] a) M. J. Antal, *Ind. Eng. Chem. Prod. Res. Dev.* **1983**, *22*, 366-375; b) R. J. Evans, T. A. Milne, *Energy Fuels* **1987**, *1*, 123-137; c) M. L. Boroson, J. B. Howard, J. P. Longwell, W. A. Peters, *AIChE J.* **1989**, *35*, 120-128; d) J. Rath, G. Staudinger, *Fuel* **2001**, *80*, 1379-1389; e) P. Morf, P. Hasler, T. Nussbaumer, *Fuel* **2002**, *81*, 843-853; f) K. Noringa, T. Shoji, S. Kudo, J. Hayashi, *Fuel* **2013**, *103*, 141-150.

[2] T. Hosoya, H. Kawamoto, S. Saka, *J. Anal. Appl. Pyrolysis* **2007**, *78*, 328-336.

[3] A. Fukutome, H. Kawamoto, S. Saka, *J. Anal. Appl. Pyrolysis* **2014**, *108*, 98-108.

[4] a) S. Glassner, A. R. Pierce, *Anal. Chem.* **1965**, *37*, 525-527; b) A. G. W. Bradbury, Y. Sakai, F. Shafizadeh, *J. Appl. Polym. Sci.* **1979**, *23*, 3271-3280; c) F. Shafizadeh, R. H. Furneaux, T. G. Cochran, J. P. Scholl, Y. Sakai, *J. Appl. Polym. Sci.* **1979**, *23*, 3525-3539; d) D. S. G. Radlein, A. Grinshpun, J. Piskorz, D. S. Scott, *J. Anal. Appl. Pyrolysis* **1987**, *12*, 39-49; e) D. Radlein, J. Piskorz, D. S. Scott, *J. Anal. Appl. Pyrolysis* **1991**, *19*, 41-63.

[5] G. J. Kwon, D. Y. Kim, S. Kimura, S. Kuga, *J. Anal. Appl. Pyrolysis* **2007**, *80*, 1-5.

[6] a) C. T. Greenwood, J. H. Knox, E. Milne, *Chemistry & Industry* **1961**, 1878-1879; bG. A. Byrne, D. Gardiner, F. H. Holmes, *J. Appl. Chem.* **1966**, *16*, 81-88; c) F. A. Wodley, *J. Appl. Polym. Sci.* **1971**, *15*, 835-851.

[7] a) A. Pictet, *Helv. Chim. Acta* **1918**, *1*, 226-230; b) J. da Silva Carvalho, W. Prins, C. Schuerch, *J. Am. Chem. Soc.* **1959**, *81*, 4054-4058; c) M. L. Wolfrom, A. Thompson, R. B. Ward, *J. Am. Chem. Soc.* **1959**, *81*, 4623-4625; d) F. Shafizadeh, C. W. Philpot, N. Ostojic, *Carbohydr. Res.* **1971**, *16*, 279-287; e) Shafizad.F, Y. Z. Lai, *J. Org. Chem.* **1972**, *37*, 278-284; f) Shafizad.F, Y. L. Fu, *Carbohydr. Res.* **1973**, *29*, 113-122; g) G. R. Ponder, G. N. Richards, *Carbohydr. Res.* **1990**, *208*, 93-104; h) E. J. Shin, M. R. Nimlos, R. J. Evans, *Fuel* **2001**, *80*, 1697-1709; i) H. Kawamoto, M. Murayama, S. Saka, *J. Wood Sci.* **2003**, *49*, 469-473; j) T. Hosoya, H. Kawamoto, S. Saka, *Carbohydr. Res.* **2006**, *341*, 2293-2297; k) T. Hosoya, H. Kawamoto, S. Saka, *J. Anal. Appl. Pyrolysis* **2008**, *83*, 64-70; l) X. Zhang, W. Yang, W. Blasiak, *J. Anal. Appl. Pyrolysis* **2012**, *96*, 110-119; m) H. Kawamoto, Y. Ueno, S. Saka, *J. Anal. Appl. Pyrolysis* **2013**, *103*, 287-292.

[8] T. Shoji, H. Kawamoto, S. Saka, *J. Anal. Appl. Pyrolysis* **2014**, *109*, 185-195.

[9] F. Shafizadeh, *J. Anal. Appl. Pyrolysis* **1982**, *3*, 283-305.

[10] X. Bai, P. Johnston, R. C. Brown, *J. Anal. Appl. Pyrolysis* **2013**, *99*, 130-136.

[11] K. Noringa, T. Shoji, S. Kudo, J.-i. Hayashi, *Fuel* **2013**, *103*, 141-150.

[12] a) W. L. Nelson, C. J. Engelder, *J. Phys. Chem.* **1925**, *30*, 470-475; b) K. Saito, T. Kakumoto, H. Kuroda, S. Torii, A. Imamura, *J. Chem. Phys.* **1984**, *80*, 4989; c) B. I. V. Tokmakov, C. C. Hsu, L. V. M. Lin, C. M, *Mol. Phys.* **1997**, *92*, 581-586; d) N. Akiya, P. E. Savage, *AIChE J.* **1998**, *44*, 405-415; e) B. Wang, H. Hou, Y. Gu, *J. Phys. Chem. A* **2000**, *104*, 10526-10528.

[13] a) E. W. R. Steacie, W. H. Hatcher, J. F. Horwood, *J. Chem. Phys.* **1935**, *3*, 291-295; b) K. Saito, T. Kakumoto, I. Murakami, *J. Chem. Phys.* **1984**, *88*, 1182-1187.

[14] a) C. H. Bamford, M. J. S. Dewar, *J. Chem. Soc.* **1949**, 2877-2882; b) P. G. Blake, G. E. Jackson, *J. Chem. Soc. B* **1968**, 1153.

[15] M. Asmadi, H. Kawamoto, S. Saka, *J. Wood Sci.* **2010**, *56*, 319-330.

[16] a) J. Piskorz, D. Radlein, D. S. Scott, *J. Anal. Appl. Pyrolysis* **1986**, *9*, 121-137; b) G. N. Richards, *J. Anal. Appl. Pyrolysis* **1987**, *10*, 251-255.

[17] a) G. M. Simmons, M. Gentry, *J. Anal. Appl. Pyrolysis* **1986**, *10*, 129-138; b) R. Bilbao, J. Arauzo, M. L. Salvador, *Ind. Eng. Chem. Res.* **1995**, *34*, 786-793; c) S. Li, J. Lyons-Hart, J. Banyasz, K. Shafer, *Fuel* **2001**, *80*, 1809-1817; d) T. Hosoya, H. Kawamoto, S. Saka, *J. Anal. Appl. Pyrolysis* **2008**, *83*, 71-77; e) D. K. Shen, S. Gu, A. V. Bridgwater, *Carbohydr. Polym.* **2010**, *82*, 39-45.

[18] a) J. C. Mackie, K. R. Doolan, *Int. J. Chem. Kinet.* **1984**, *16*, 525-541; b) N. Leplat, J. Vandooren, *Combust. Flame* **2012**, *159*, 493-499.

[19] Y. S. Stein, M. J. Antal Jr, M. Jones jr, *J. Anal. Appl. Pyrolysis* **1983**, *4*, 283-296.

[20] R. G. Graham, L. K. Mok, M. A. Bergougnou, H. I. De Lasa, B. A. Freel, *J. Anal. Appl. Pyrolysis* **1984**, *6*, 363-374.

[21] A. Fukutome, H. Kawamoto, S. Saka, *unpuplished data*.

[22] a) I. Pastorova, R. E. Botto, P. W. Arisz, J. J. Boon, *Carbohydr. Res.* **1994**, *262*, 27-47; b) X. Zhang, J. Golding, I. Burgar, *Polymer* **2002**, *43*, 5791-5796; c) M. M. Titirici, M. Antonietti, N. Baccile, *Green Chem.*

2008, *10*, 1204; d) N. Baccile, G. Laurent, F. Babonneau, F. Fayon, M. M. Titirici, M. Antonietti, *J. Phys. Chem. C* **2009**, *113*, 9644-9654; e) C. Falco, F. Perez Caballero, F. Babonneau, C. Gervais, G. Laurent, M. M. Titirici, N. Baccile, *Langmuir* **2011**, *27*, 14460-14471.

[23] H. Kawamoto, T. Hosoya, Y. Ueno, T. Shoji, S. Saka, *J. Anal. Appl. Pyrolysis* **2014**, *109*, 41-46.

[24] S. Matsuoka, H. Kawamoto, S. Saka, *J. Anal. Appl. Pyrolysis* **2012**, *93*, 24-32.

[25] a) O. Boutin, M. Ferrer, J. Lédé, *J. Anal. Appl. Pyrolysis* **1998**, *47*, 13-31; b) O. Boutin, M. Ferrer, J. Lédé, *Chem. Eng. Sci.* **2002**, *57*, 15-25;

c) S. Matsuoka, H. Kawamoto, S. Saka, *J. Anal. Appl. Pyrolysis* **2014**, *106*, 138-146.

[26] a) M. A. Grela, V. T. Amorebieta, A. J. Colussi, *J. Phys. Chem.* **1985**, *89*, 38-41; b) M. A. Grela, A. J. Colussi, *J. Phys. Chem.* **1986**, *90*, 434-437.

[27] T. Hosoya, H. Kawamoto, S. Saka, *J. Anal. Appl. Pyrolysis* **2009**, *85*, 237-246.

Entry for the Table of Contents (Please choose one layout)

Layout 1:

FULL PAPER

Towards coke-/tar-free gasification: Gaseous levoglucosan (LG) was gasified cleanly without forming any dehydration products (coke, furans, and aromatics). Coking occurred upon cooling of LG to form the molten phase, in which intermolecular hydrogen bonding serves as an acid catalyst to promote dehydration.
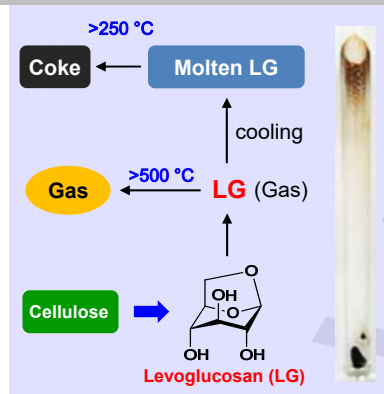
Asuka Fukutome, Haruo Kawamoto, and Shiro Saka[a]*

Page No. – Page No.

Uncovering the gas-, tar- and coke-forming processes in cellulose gasification from the gas phase reactions of levoglucosan as an intermediate